



Advances in Research

19(2): 1-10, 2019; Article no.AIR.48955
ISSN: 2348-0394, NLM ID: 101666096

Grid-connected Response Verification of AC Microgrid under Single Line-to-ground Short Circuit

Maruf A. Aminu^{1*}

¹Department of Electrical and Electronics Engineering, Faculty of Engineering, Nile University of Nigeria, Abuja, Nigeria.

Author's contribution

The sole author designed, analysed, interpreted and prepared the manuscript.

Article Information

DOI: 10.9734/AIR/2019/v19i230117

Editor(s):

(1) Dr. Omveer Singh, Department of Electrical Engineering, School of Engineering, Gautam Buddha University, India.

Reviewers:

(1) Bharat Raj Singh, Dr. A. P. J. Abdul Kalam Technical University, India.

(2) Hachimenum Amadi, Federal University of Technology, Nigeria.

(3) Raheel Muzzammel, University of Lahore, Pakistan.

Complete Peer review History: <http://www.sdiarticle3.com/review-history/48955>

Received 24 February 2019

Accepted 11 May 2019

Published 05 June 2019

Original Research Article

ABSTRACT

In design of power systems, assumptions are made to model the physical systems. The assumptions may not sufficiently reflect the behavior of the system under normal and faulted conditions. Under short circuit conditions, system parameters vary significantly, particularly in microgrids with grid interconnection capabilities. This paper presents the result of validating the response of a microgrid which is capable of grid interconnection and islanding under voltage and reactive power control regimes. The microgrid is modeled to incorporate two wind turbines, each rated 5.5 kW, 400 V. The utility has synchronous generator rated 100 MW, 13.8 kV. Both the utility and microgrid are capable of exchanging active power and reactive power. Single line-to-ground short circuits are introduced and withdrawn at 30.00 s and 32.00 s, respectively. The dynamic responses of the testbed are captured pre-, during- and post-short circuit in grid-connected mode under both control regimes. The response of the testbed is verified to be consistent with established short circuit theory, verifying the validity of the system for short circuit detection and analysis. The testbed can therefore be used for short circuit and related studies, design optimization and power system performance prediction.

Keywords: Microgrid; short circuit; grid-connected; active power; reactive power.

*Corresponding author: E-mail: maruf.aminu@gmail.com;

1. INTRODUCTION

Power systems require optimal operation in order to meet declared demand and system losses. In addition to input variables, the yield from a power system depends on the frequency of shut down occasioned by scheduled maintenance and abnormal conditions such as short circuits [1]–[3]. In a microgrid, the most frequent short circuit is single line-to-ground (see Fig. 1) [4]. Generally, short circuits result in low impedance and progressive insulation failure and consequent system damage if the short circuit is not interrupted speedily. For optimum system operation, control and protective devices are required. While control devices monitor system variables in order to make control decisions depending on preset values [5], protective devices monitor system variables in order to isolate requisite sections of the system when conditions dictate [6,7]. Protective devices are employed to detect and isolate the minimum faulted segment of the system. A protective device includes two components: detection and isolation networks. The detection network detects onset of abnormal conditions while the isolation network isolates the minimum faulted segment of the power system so as to minimize interruption of service to the consumer. Specific functions of protective devices include:

- (i) Minimizing damage and repair cost in the event of a fault in the system.
- (ii) Safeguarding the system to ensure supply continuity.
- (iii) Safety of system personnel [8–12].

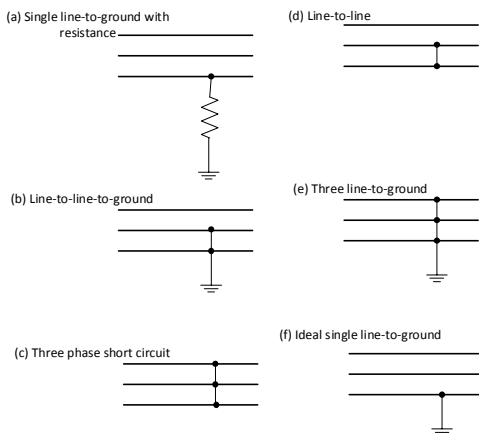


Fig. 1. Simple classification of short circuits

2. MOTIVATION

Statutorily, every protective device is expected to have high reliability, low cost, high speed of

response, capability to distinguish between normal and abnormal segments of the power system, and have sufficient sensitivity to faults [13]. This work is motivated by the need to ensure that the testbed is valid for system studies. This paper therefore presents verification of the responses of the microgrid testbed to single line-to-ground short circuit in grid-connected mode under voltage and reactive power control regimes using dynamic analysis. Dynamic analysis depicts the sub-transient, transient and steady-state variation of critical parameters of the system [14]. Design of engineering systems require performance prediction and optimization using system models [15–18].

3. MODELING OF THE SYSTEM

The testbed is modeled to operate under two control strategies; voltage (V) and reactive power (Q) controls. While the controller maintains 4% droop under V control, it maintains constant reactive power at the grid under Q control even when the system is stressed with short circuit(s). The microgrid consists of two wind turbines (WTs) as microsources servicing two local loads. Each WT is nominally rated 5.5 kW and is connected to the utility at the point of common coupling (PCC) via a distribution feeder (see Fig. 2). The PCC allows exchange of resources (active power and reactive power) between the utility and the microgrid. The three-phase stator voltage of each WT is transformed to stationary dc reference frame using Edith Clarke's transformer presented in equation (1). A multivariable fuzzy rule-based (MFR) relay is modeled using two sub-relays: microsource sub-relay and feeder sub-relay. The MFR relay is embedded for detection of single line-to-ground (SLG) short circuit (SC) and consequent tripping of requisite circuit breaker.

$$v_{\alpha\beta\gamma}(t) = \frac{2}{3} \begin{bmatrix} 1 & -\frac{1}{2} & -\frac{1}{2} \\ 0 & \frac{\sqrt{3}}{2} & -\frac{\sqrt{3}}{2} \\ \frac{1}{2} & \frac{1}{2} & \frac{1}{2} \end{bmatrix} \begin{bmatrix} v_a(t) \\ v_b(t) \\ v_c(t) \end{bmatrix} \quad (1)$$

where,

$v_{\alpha\beta\gamma}(t)$ is a vector representing the α , β and γ components of the transformed voltage.

$v_a(t)$, $v_b(t)$ and $v_c(t)$ represent components of voltage in abc reference frame.

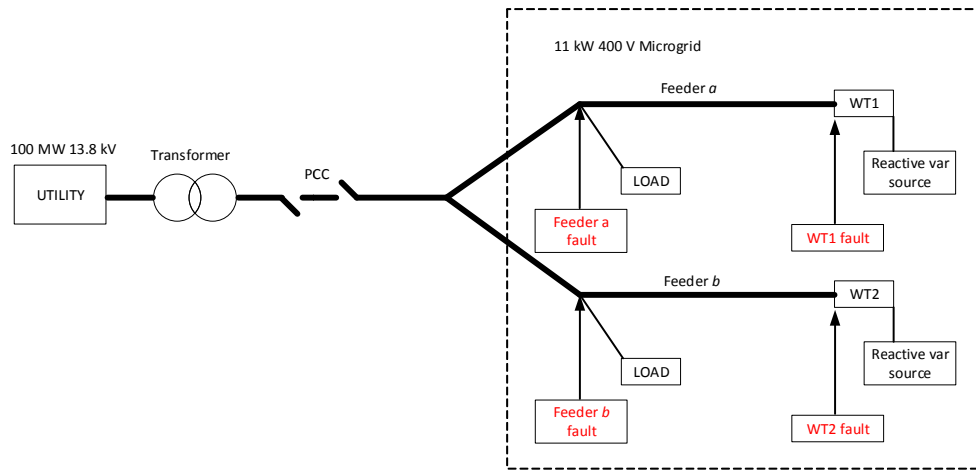


Fig. 2. Major elements of the modeled system shown in block diagram

4. RESULTS

4.1 Simulation of Short Circuits and System Responses

Fig. 3 presents the nominal response of WT1 during normal operation in grid-connected mode under both control strategies. In the figure, the three-phase active power [P(W)] in Watts and three-phase reactive power [Q(var)] in var are presented.

Fig. 3 presents response of WT1 under normal operating conditions. Note that the active power generated is 92% of nominal rating due to the prevailing wind input at 50.00 simulation second. In both control regimes, the reactive power absorption at 50.00 second is less than 20 var. Response of the microsource sub-relay is 1

(open) between 0 to 9.0 simulation seconds and 0 (closed) thereafter. The initial open response of the MFR sub-relay is occasioned by high initial starting current of both WT1 and the synchronous generator in the utility. This could be prevented by modeling a 10-second delay in the MFR sub-relay.

When the PCC is closed to allow grid interconnection for exchange of resources, phase-a SLG SC is applied at 30.00 seconds and withdrawn at 32.00 seconds. The dynamic response of the system depicting sub-transient, transient and steady-state is captured. During these states, the three phase WT1 stator voltage in stationary dc reference frame and currents under SLG SC, in both voltage and reactive power control regimes, are presented (Fig. 4 to Fig. 14).

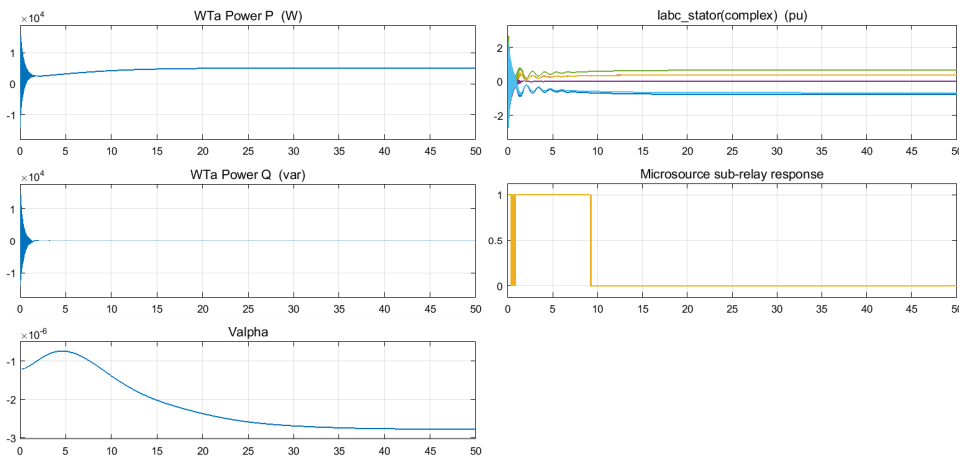


Fig. 3. Normal response of WT1 under V and Q controls

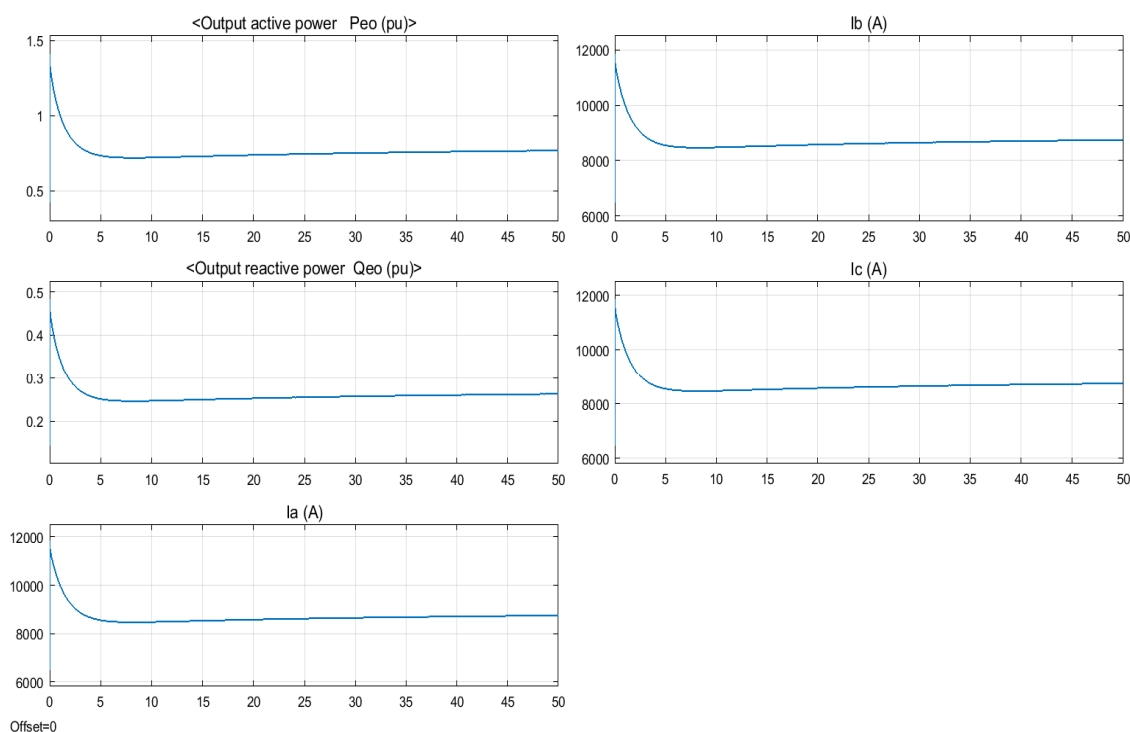


Fig. 4. Response of utility to SLG SC applied at terminals of WT1 in the microgrid

Fig. 4 presents response of the utility to SLG SC in the microgrid. Observe that the per unit active power, per unit reactive power, and phase currents are unperturbed by the disturbance in the microgrid due to the large inertia in the utility. This indicates that the utility provides low voltage ride-through (LVRT) support to the microgrid [19,20].

In Figs. 5 and 6, both active power and reactive power are unperturbed by the short circuit in both control regimes due to the support from the utility since the system is in grid-connected mode. However, the alpha component of the voltage is disrupted, resulting in *open* response from the MFR sub-relay during SC. In both figures, the feeder sub-relay responds with a 0 (*open*), indicating *selectivity* between microsource sub-relay and feeder sub-relay in response to microsource SC.

When the microgrid is grid-connected and the large-inertia utility generator is stressed with SLG SC, it provokes frequency oscillation and large voltage drop in the utility resulting in reactive power oscillation in the microgrid under V control regime (Fig. 9). Under the same stress condition

but in reactive power control regime, the reactive power source in the microgrid is able to support it through the stress, resulting in non-response of the microsource sub-relay (Fig. 10).

Contrary to the response obtained in Figs. 9 and 10, when similar utility SC is applied, the feeder responds with virulent oscillation of critical parameters in both control regimes (Figs. 11 and 12). The feeder lacks reactive power management components, resulting in high-severity oscillation of the critical parameters with a potential for sustained oscillation in both control regimes.

When the grid-connected microgrid is subjected to cross-country (both microgrid and utility disturbance) SLG SC, the WT1 responds with sustained oscillation of reactive power at the onset of SC in voltage control regime (Fig. 13). In reactive power control regime, the WT1 responds with reactive power compensation sufficient to dampen oscillation and maintain steady-state operation during- and post-SC (Fig. 14). In this control regime the voltage is perturbed, resulting in detection by the microsource sub-relay.

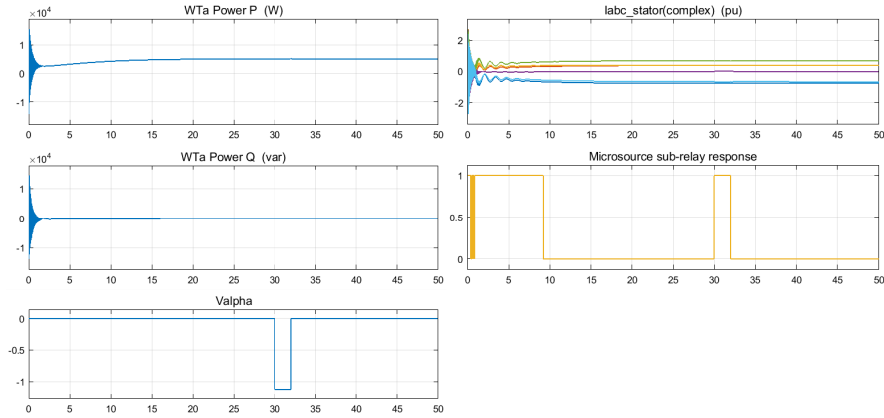


Fig. 5. Response of the WT1 and associated devices when SLG SC is applied at WT1 from 30.00 s to 32.00 s (V control)

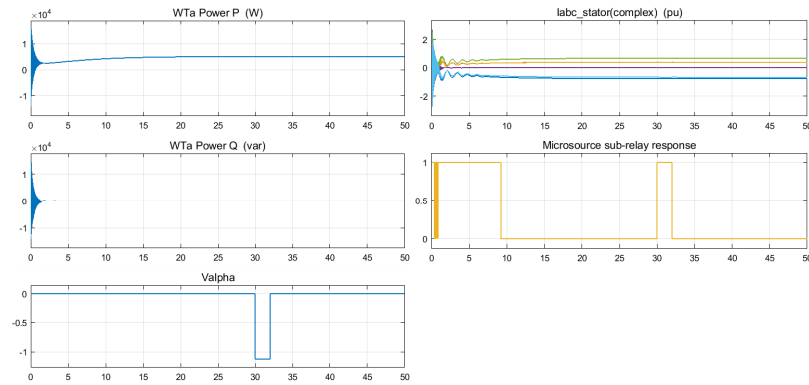


Fig. 6. Response of the WT1 and associated devices when SLG SC is applied at WT1 from 30.00 s to 32.00 s (Q control)

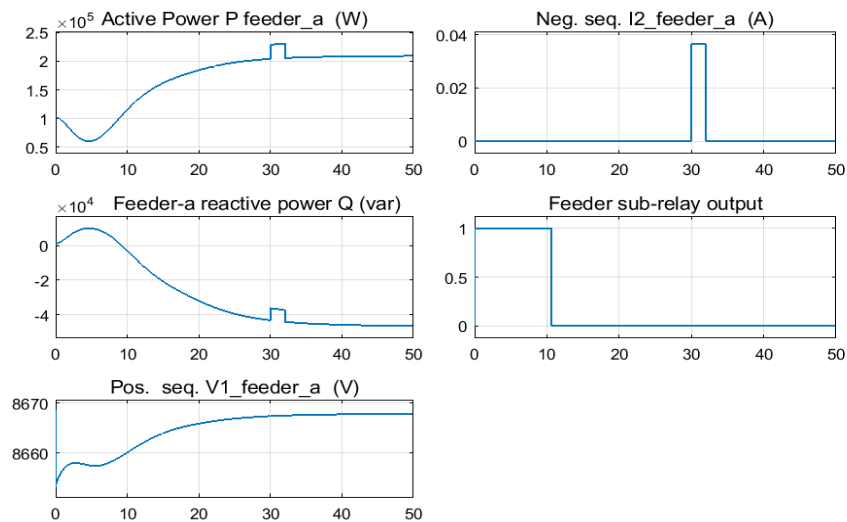


Fig. 7. Response of feeder-a to SLG SC at terminals of WT1 (V control)

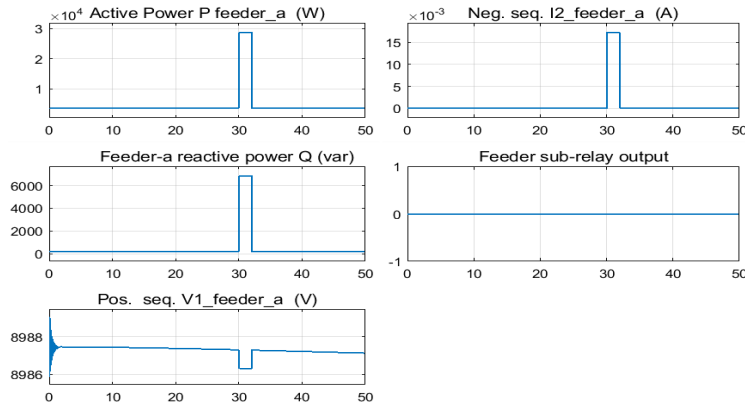


Fig. 8. Response of feeder-a to SLG SC at terminals of WT1 in islanded mode (Q control)

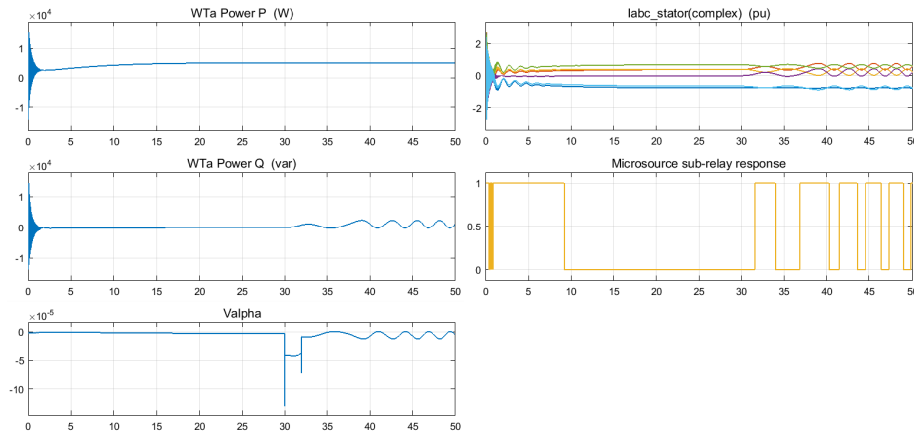


Fig. 9. Response of the WT1 and associated devices when SLG SC is applied at utility generator terminal from 30.00 s to 32.00 s (V control)

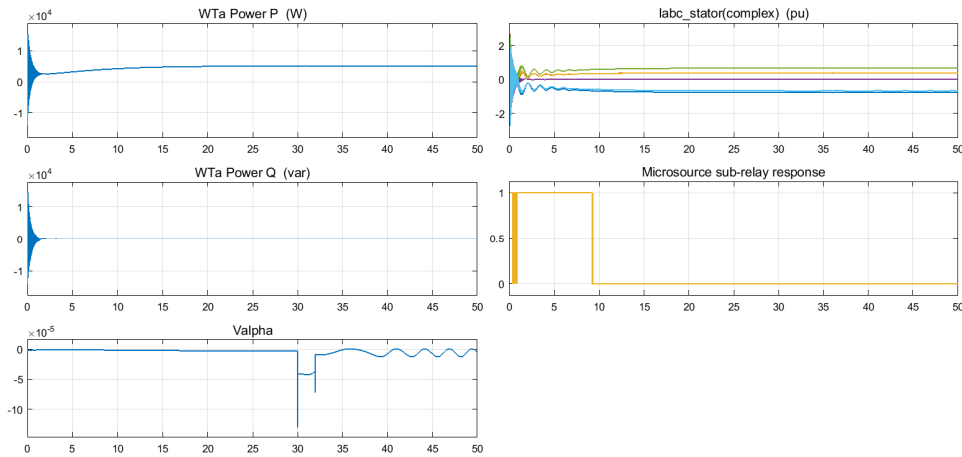


Fig. 10. Response of the WT1 and associated devices when SLG SC is applied at utility generator terminal from 30.00 s to 32.00 s (Q control)

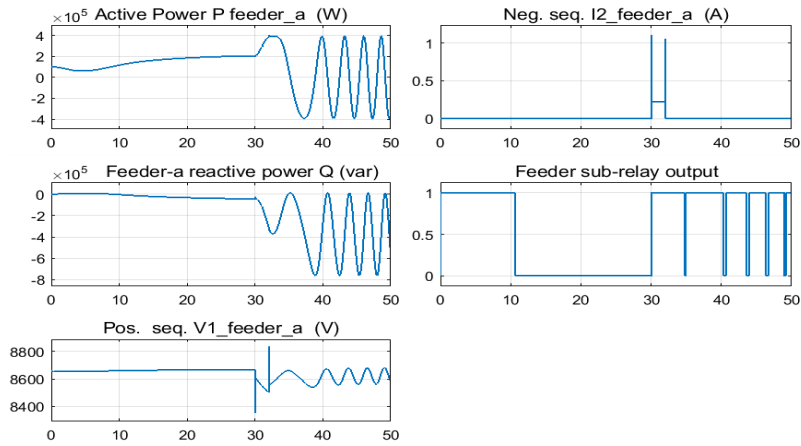


Fig. 11. Response of feeder-a to SLG SC at terminal of utility generator (V control)

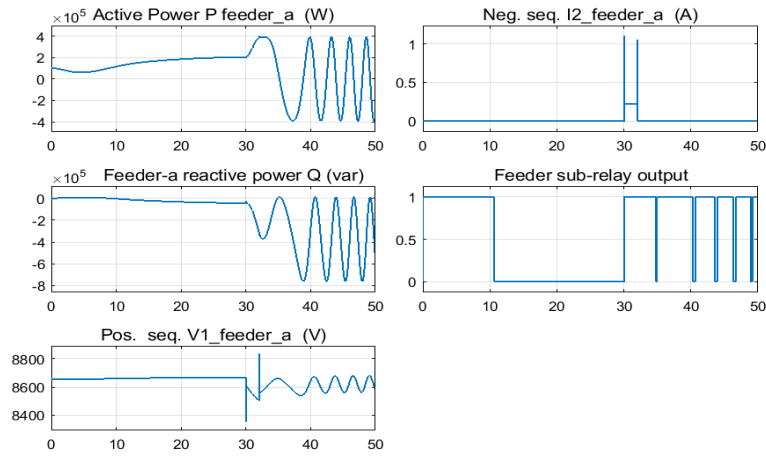


Fig. 12. Response of feeder-a to SLG SC at terminal of utility generator (Q control)

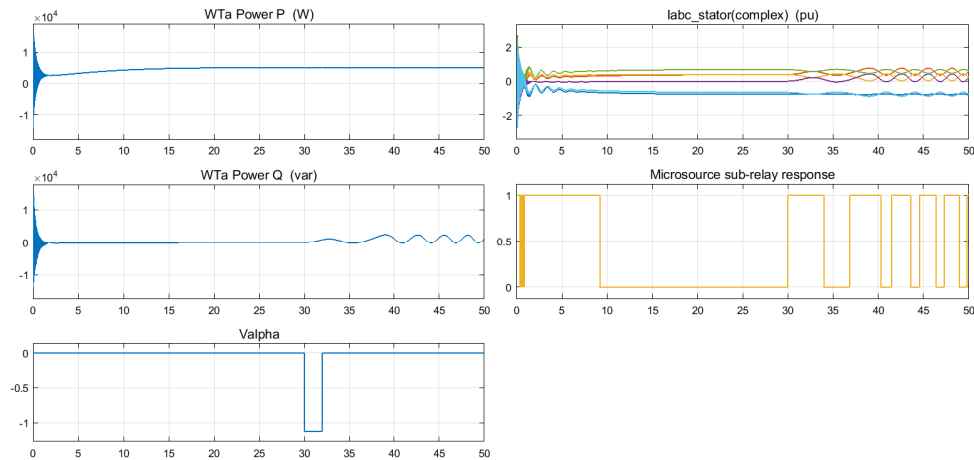


Fig. 13. Response of the WT1 and associated devices when SLG SC cross-country is applied at utility-microgrid generator terminals from 30.00 s to 32.00 s (V control)

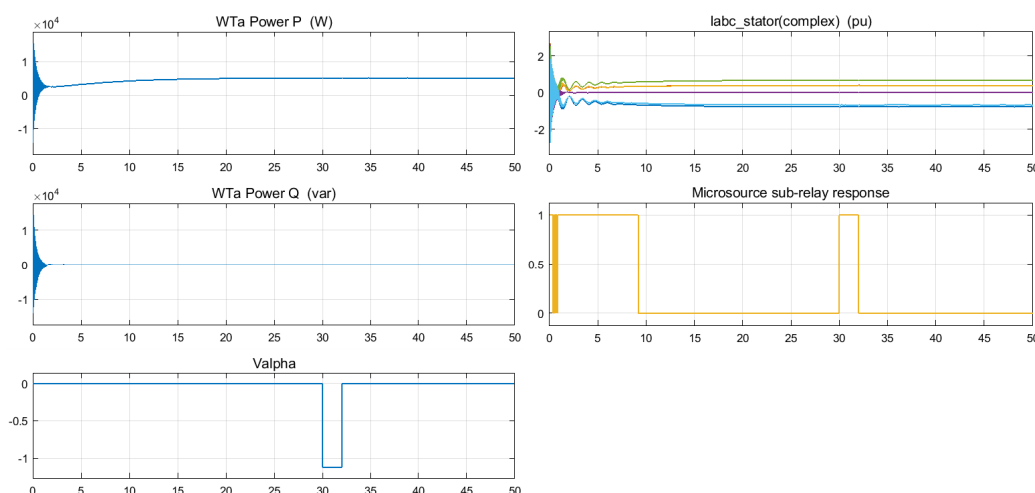


Fig. 14. Response of the WT1 and associated devices when SLG SC cross-country is applied at utility-microgrid generator terminals from 30.00 s to 32.00 s (Q control)

5. DISCUSSION

In stress-free operating condition, WT1 or WT2 generates 5.114 kW which represents 92% of its nominal active power, independent of control regime. Generally, reactive power demand is more in V control than in Q control, indicating that the internal capacitor bank of each WT supports its reactive demand. This is indicative of superior reactive power management under Q control than under V control. In Figs. 5 and 6, both active power and reactive power are unperturbed by the short circuit in both control regimes due to the support from the utility since the system is in grid-connected mode. However, the alpha component of the voltage is disrupted, resulting in *open* response from the MFR sub-relay during SC. The post-SC response of the relay *closes* requisite circuit breaker (circuit breaker is not modeled in this work). The utility support enables the microgrid to ride through attending frequency oscillation and low voltage occasioned by the short circuit stress. When the utility support is withdrawn, the microgrid exhibits perturbation to SC stress in islanded mode (Figs. 7 and 8). In both figures, the feeder sub-relay responds with a 0 (*open*), indicating *selectivity* between microsource sub-relay and feeder sub-relay in response to microsource SC.

In Fig. 13 when the grid-connected microgrid is subjected to cross-country SLG SC, the WT1 responds with sustained oscillation of reactive power at onset of SC in voltage control regime. However, in reactive power control regime, the

WT1 responds with reactive power compensation (from its reactive var source) sufficient to dampen oscillation and maintain steady-state operation during- and post-SC (Fig. 14). In this control regime the voltage is perturbed, resulting in detection by the microsource sub-relay [21]–[24].

6. CONCLUSION

The testbed under validation in this work is modeled to operate under two control regimes. The testbed is investigated to examine performance of the utility-enabled microgrid under both normal and faulted operating conditions. The results of tests conducted by simulating 2-second single line-to-ground short circuit shows that the four critical parameters vary in a manner and magnitude that is consistent with short circuit theories. In both control strategies, active power is disrupted when under short circuit, indicating stress on both the wind turbine and the synchronous generator. The reactive power responds with improved performance under reactive power control regime than under voltage control regime, indicative of validity of the testbed. Similarly, the dynamic response of current and voltage parameters typifies real power system response under stress. Thus, dynamic response of the testbed is determined pre-, during- and post-short circuit under both control regimes. The response is shown to be consistent, symptomatic of a valid testbed suitable for short circuit analysis in a microgrid capable of grid connection. The result

of this study shows that the dynamic response of the testbed to single line-to-ground short circuits is therefore verified to be valid and consistent with established short circuit theory.

COMPETING INTERESTS

Author has declared that no competing interests exist.

REFERENCES

1. Didier G, Bonnard CH, Lubin T, Lévêque J. Comparison between inductive and resistive SFCL in terms of current limitation and power system transient stability. *Electric Power Systems Research*. 2015; 125:150–158.
2. Papaefthymiou SV, Lakiotis VG, Margaritis ID, Papathanassiou SA. Dynamic analysis of island systems with wind-pumped-storage hybrid power stations. *Renewable Energy*. 2015;74:544–554.
3. Rona B, Güler Ö. Power system integration of wind farms and analysis of grid code requirements. *Renewable and Sustainable Energy Reviews*. 2015;49:100–107.
4. Weedy BM, Cory BJ, Jenkins N, Ekanayake JB, Strbac G. *Electric power systems*. 5th ed. Somerset, NJ, USA: John Wiley & Sons; 2012.
5. MA Aminu. Design of reactive power and voltage controllers for converter-interfaced ac microgrids. *British Journal of Applied Science & Technology*. 2016;17:1.
6. Sulla F, Svensson J, Samuelsson O. Symmetrical and unsymmetrical short-circuit current of squirrel-cage and doubly-fed induction generators. *Electric Power Systems Research*. 2011;81(7):1610–1618.
7. MA Aminu. Modeling and simulation of protective relay for short circuits in AC micro-grids using fuzzy logic. Curtin University, Perth, Australia; 2016.
8. Chaudhary M, Brahma SM, Ranade SJ. Validated short circuit modeling of type 3 wind turbine generator with crowbar protection. Presented at the North American Power Symposium (NAPS). 2013;1–6.
9. Roennspiess OE, Efthymiadis AE. A comparison of static and dynamic short circuit analysis procedures. *IEEE Transactions on Industry Applications*. 1990;26(3):463–475.
10. Soni N, Doola S, Chandorkar MC. Improvement of transient response in microgrids using virtual inertia. *IEEE Transactions on Power Delivery*. 2013;28(3):1830–1838.
11. Palizban O, Kauhaniemi K, Guerrero JM. Microgrids in active network management – part II: System operation, power quality and protection. *Renewable and Sustainable Energy Reviews*. 2014;36:440–451.
12. Patrao I, Figueres E, Garcerá G, González-Medina R. Microgrid architectures for low voltage distributed generation. *Renewable and Sustainable Energy Reviews*. 2015;43:415–424.
13. Schomaker J. Overcurrent protective devices preserve system integrity. *Plant Engineering*. 2005;59(6):48–54.
14. Aminu MA. Validating response of AC micro-grid to three phase short circuit in grid-connected mode using dynamic analysis. *International Journal of Electrical Components and Energy Conversion*. 2016;2(4):21–34.
15. Tchakoua P, Wamkeue R, Ouhrouche M, Tameghe TA, Ekemb G. A new approach for modeling darrieus-type vertical axis wind turbine rotors using electrical equivalent circuit analogy: Basis of theoretical formulations and model development. *Energies* (19961073). 2015;8(10):10684–10717.
16. K P'yankov, M Toporkov. Mathematical modeling of flows in wind turbines with a vertical axis. *Fluid Dynamics*. 2014;49(2): 249–258.
17. Bazilevs Y, Korobenko A, Deng X, Yan J. Novel structural modeling and mesh moving techniques for advanced fluid-structure interaction simulation of wind turbines. *International Journal for Numerical Methods in Engineering*. 2015; 102(3/4): 766–783.
18. Xu F, Yuan FG, Liu L, Hu J, Qiu Y. Performance prediction and demonstration of a miniature horizontal axis wind turbine. *Journal of Energy Engineering*. 2013;139(3):143–152.
19. Akhmatov V. Full-scale verification of dynamic wind turbine models in *Wind Power in Power Systems*, John Wiley & Sons, Ltd. 2012;865–889.
20. Dongliang X, Zhao X, Lihui Y, Ostergaard J, Yusheng X, Kit Po W. A comprehensive LVRT control strategy for DFIG wind turbines with enhanced reactive

- power support. IEEE Transactions on Power Systems. 2013;28(3):3302–3310.
21. Li J, Zheng T, Wang Z. Short-circuit current calculation and harmonic characteristic analysis for a doubly-fed induction generator wind turbine under converter control. Energies (19961073). 2018;11(9):2471.
 22. Sellami T, Berriri H, Jelassi S, Darcherif AM, Mimouni MF. Short-circuit fault tolerant control of a wind turbine driven induction generator based on sliding mode observers. Energies (19961073). 2017;10(10):1611.
 23. MA Eftekhari, AS Molavi Tabrizi, SM Sadeghzadeh. The effect of resistive-type superconducting fault current limiters on the test feeder with wind-turbine generation system. IETE Journal of Research. 2012;58(5):411–417.
 24. XY Zheng, Y Lei. Stochastic response analysis for a floating offshore wind turbine integrated with a steel fish farming cage. Applied Sciences (2076-3417). 2018;8(8):1229.

© 2019 Aminu; This is an Open Access article distributed under the terms of the Creative Commons Attribution License (<http://creativecommons.org/licenses/by/4.0>), which permits unrestricted use, distribution, and reproduction in any medium, provided the original work is properly cited.

Peer-review history:

*The peer review history for this paper can be accessed here:
<http://www.sdiarticle3.com/review-history/48955>*